Supplementary information to:

Sustained fetal hematopoiesis contributes to juvenile death in leukemia: evidence from a dual-age-specific mouse model

Nitza Vara[1#], Yuqing Liu[2#], Yan Yan[1], Shelly Y. Lensing[1,3], Natalia Colorado[1], Delli Robinson[1], Jingliao Zhang[1], Xin Zhang[4], Erich A. Peterson[1], Nicholas J. Baltz[1], Daohong Zhou[4], Alice Bertaina[6], Donald J. Johann, Jr[1]., Peter D. Emanuel[1,5]*, and Y. Lucy Liu[1,6]*

Supplemental materials and methods

Study design and mice

Founder mice bearing *Pten*$^{floxP/floxP}$ (*Pten*$^{fl/fl}$, B6.129S4-*Pten*$^{tm1\ Hwu}$/J), *Nf1*$^{Fcr/+}$ (B6.129S6-*Nf1*^{tm1Frc}/J), *Nf1*$^{floxP/floxP}$ (*Nf1*$^{fl/fl}$, B6.129 [Cg]-*Nf1*$^{tm1\ Par}$/J), and *Mx1-Cre* (B6.Cg-Tg [*Mx1-Cre*]1Cgn/J) were purchased from The Jackson Laboratory. We produced the experimental mice with desired genotypes by crossbreeding as previously reported (Supplemental figure 1).[1] *Pten* deletion and *Nf1* LOH were induced by intraperitoneal injection of 30μL of polyinosinic-polycytidylic acid (*pIpC*) at a concentration of 1μg/μL in normal saline (InvivoGen), on postnatal day 8 and 10 (hereafter referred collectively as PND8, supplemental Figure 1A). Mouse-tails were clipped at age PND15 and genotyping was performed following instructions provided by the vendor. Animals were included once they were enrolled when they had genotype-matched littermates. No mice were excluded unless their death was caused by accidents, such as wounds because of fighting or cage flooding. The experimental procedures were approved by the Institutional Animal Care and Use Committee at the University of Arkansas for Medical Sciences (UAMS).

Histological analysis

Mice were euthanized at an age of 17-19 days for juvenile groups or 3-4 months for adult groups. Femurs, tibias, spleen, liver, lung, and intestine/colon were collected and fixed in 10% buffered formalin (Thermo Fisher Scientific Inc.). Paraffin-embedded tissue sections were prepared and stained with hematoxylin and eosin stain (HE) by the UAMS Experimental Pathology Core Lab. Images were acquired with an Aperio CS2 scanner, and analyzed by ImageScope (Leica Biosystems).

Hematopoietic cell profiling

Peripheral blood (PB) was collected from the retro-orbital venous sinus. Twenty μL aliquots were analyzed for complete blood counts (CBC) by a Vet Abc Hematological Analyzer (scil Animal Care Co.). White blood cell differentials were manually counted from blood smears stained with StainRITE® May-Grünwald-Giemsa (MGG, Polysciences, Inc.). Bone marrow (BM) cells were collected by flushing the femurs and tibias with Ca^{++}- and Mg^{++}-free phosphate buffered saline (PBS) containing 1% fetal calf serum (FCS, Hyclone Laboratories). Single cells suspensions were prepared by gently passing the cells through a FALCON® cell-strainer with 35μm pore size (Corning Incorporated). Single spleen cells were collected by crushing one third of the spleen tissue with a pestle in PBS-1% FCS, and filtering through a cell strainer with 70μm pore size (BD Biosciences). Single cells from BM were centrifuged on slides with Cytospin® 3 cell preparation system (Shandon Scientific Ltd.) and stained with MGG.

Flow cytometric analysis

Single cell suspensions were prepared from BM or spleen, and 100μl of PB after red cell lysis with lysis buffer (0.15 M NH_4Cl, 10mM $KHCO_3$, 0.1mM EDTA, pH 7.4).[2] The nucleated cells were washed twice in PBS-1% BSA-1mM EDTA. Cells ($0.5x10^6$/test) were blocked with anti-CD16/CD32 antibodies before staining with specific antibodies (Supplemental Table 1). Data were acquired by Accuri C6 or LSRII with FACSDiva (BD Biosciences) and analyzed by FlowJo software V10.1.5 (Tree Star, Inc.).

Isolation of bone marrow lineage-negative hematopoietic cells (Lin− cells), HSCs and LT-HSCs

BM mononuclear cells (MNCs) were isolated from BM nucleated cells by using density gradient centrifugation with Histopaque®-1083 (Sigma). Lineage-negative hematopoietic cells (Lin^-, including Gr1, CD3e, B220, and Ter119) were purified by magnetic-activated cell sorting (MACS) using Dynabeads Biotin Binder (Invitrogen) following the manufacturer's instructions. LT-HSCs ($Lin^-Sca1^+cKit^+CD48^-CD150^+CD34^-CD135^-$) were further sorted by an Aria II cell sorter (BD Biosciences) as described previously.[3] Information for antibodies are available in Supplemental Table 1. Data were analyzed by FlowJo software V10.1.5.

Colony-forming unit-granulocyte-macrophage (CFU-GM) assay

CFU-GM assays were performed with a modified protocol as previously described.[4] Briefly, unfractionated BM nucleated cells (WBM) were cultured overnight at a density of $0.8x10^6$/mL in RPMI-1640 medium (Fisher Scientific Inc.) with 10% FCS, 2ng/mL of recombinant mouse GM-CSF (rmGM-GSF) and interleukin-3 (rmIL-3) (R & D Systems). Suspended cells were collected and washed once in PBS, then starved in RPMI-1640 with 0.5% BSA for 4 hours. Triplicate 1-ml semi-solid cultures with 10^5/mL MNCs were seeded in 35-mm plates in 0.3% agar and McCoys' 5A medium (Sigma Chemical Co.) supplemented with nutrients and 15% fetal bovine serum. rmGM-CSF or rmIL-3 was added at the time when the cultures were initiated. After 7 days of incubation in 5% CO_2 at 37°C, CFU-GM colonies were enumerated with a colony defined as a minimum of 40 cells.

Competitive bone marrow transplantation (BMT)

Competitive BMT was performed as previously reported.[1] Briefly, adult C57BL/6 recipient mice with $CD45.1^+$ background at age 6-8 weeks (Jackson Laboratory) were lethally irradiated with a single-dose of 9.5Gy delivered by a Mark I ^{137}Ce γ–irradiator with a rotating platform (JL Shepherd and Associates, Glendale, CA).

WBM cells were collected from juvenile diseased donor mice with *Pten*Δ/Δ*Nf1*^{LOH} and littermates or adult donors with *Pten*$^{+/\Delta}$*Nf1*^{LOH} when they were moribund. Age-matched WBM cells from wild-type (WT) controls ($2x10^5$) or diseased mice ($0.2\text{-}1x10^6$) with CD45.2$^+$ background were mixed with $2x10^5$ rescue cells from WT CD45.1$^+$ mice, respectively. Donor cells were suspended in 120μL of PBS-5% mouse serum and injected into the retro-orbital venous sinus of irradiated recipient mice at 6 hours post-irradiation. Transplanted recipient mice were maintained with regular mouse chow and sterile water without additives. Four weeks (wks) after BMT, peripheral blood (PB) was collected from recipient mice serially at 4-week intervals for complete blood count (CBC) and flow cytometry analysis (supplemental Figure 8A). Recipient mice were collected and processed for final evaluation at 10-18 wks post-transplant for donor-derived hematopoiesis as previously reported.[1]

Serial single-cell transplantations

In primary single LT-HSC transplants, single LT-HSC from donor mice was freshly sorted into each well of a 96-well plate, in which $2x10^5$ rescue cells from BM of WT CD45.1$^+$ mice were prepared with 120μL of PBS-5% mouse serum, and then injected into the retro-orbital venous sinus of irradiated recipient mice at 6 hours post-irradiation as described in Competitive BMT. For secondary and tertiary single LT-HSC transplants, donor-derived single LT-HSC with CD45.2$^+$ was sorted from primary or secondary recipient mice 16 weeks post primary or secondary transplants, respectively (supplemental Figure 11). Transplanted recipient mice were maintained as described in Competitive BMT. Blood, BM, and spleens from recipient mice were collected and evaluated as described in Competitive BMT.

Blood reconstitution analysis

Peripheral blood was collected from retro-orbital venous sinus of BMT recipients into EDTA-coated Eppendorf tubes (Fisher Scientific). Twenty μL aliquots were analyzed for white blood count (WBC) and 100μL was used for analyses of donor-derived progenies by flow cytometry. CD45.2 positivity was used as a

marker for donor-derived cells. In single-HSC transplants, recipient mice were considered to be reconstituted by donor LT-HSC when donor-derived myeloid ($CD45.2^+CD11b^+$) and lymphoid lineage (sum of $CD45.2^+B220^+$ and $CD45.2^+CD3e^+$) was >0.1% of WBC in recipient mice.

Cell lysate preparation and western blot

Whole BM cells were collected from femurs/tibias and cultured overnight at a density of $0.8x10^6$/ml in RPMI-1640 medium (Fisher Scientific Inc.) with 10% FCS, 2ng/ml of rmGM-CSF and rmIL-3. After being washed in PBS once, cells were starved in RPMI-1640 with 0.5% BSA for 4 hours, then stimulated for 30 minutes in RPMI-1640 with 0.5% BSA and 10pM of rmGM-CSF before being lysed in a density of $2x10^7$/mL in 2x Laemmli sample buffer (Bio-Rad Laboratory). Samples were stored in aliquots in -80°C for further analysis. Western blots were performed as previously reported.[4,5] Details for antibodies are listed in Supplemental Table 2.

RNA-seq sample processing and NGS

BM Lin^- cells were prepared by MACS from WT and JMML-diseased littermate mice at age PND17, and were lysed immediately in DNA/RNA lysis buffer. Total RNA was isolated using the Quick-DNA/RNA MiniPrep Plus Kit (Zymo Research, catalog number D7003) following manufacturer recommendation with on-column DNase I treatment. The Qubit Broad-Range RNA Assay Kit (Thermo Fisher Scientific, catalog number Q10211) was used to quantify preps and the Fragment Analyzer Standard-Sensitivity RNA Analysis Kit (Agilent, catalog number DNF-471-0500) was used to assess RNA integrity.

RNA-seq samples were prepared using the TruSeq Stranded Total RNA Library Prep Gold kit (Illumina, catalog number 20020599) according to manufacturer recommendation. Starting with 250ng of total RNA, ribosomal RNA was depleted, followed by fragmentation, cDNA synthesis, adapter-ligation of IDT for Illumina – TruSeq RNA UD Indexes (catalog number 20022371), and purification with AMPure XP beads (Beckman Coulter, catalog number A63881). Libraries were assessed using the Fragment Analyzer high-sensitivity NGS

fragment gel kit (Agilent, catalog number DNF-474-0500), the Qubit 1X dsDNA HS Assay Kit (Thermo Fisher Scientific, catalog number Q33231), and the KAPA Universal Library Quantification Kit (Roche, catalog number KK4824). Libraries were then denatured and diluted with 1% PhiX beginning with a 3nM pool of libraries following the standard ExAmp protocol and clustered on a HiSeq 3000/4000 PE flow cell. Paired-end sequencing was performed on an Illumina HiSeq 3000 with a 150-cycle SBS kit at 2x75 to yield an average of approximately 129 million mapped reads per sample.
Raw data are available at https://www.ncbi.nlm.nih.gov/geo/query/acc.cgi?acc=GSE137152.

RNA-seq data pipeline analysis

RNA-seq samples were first demultiplexed and FastQ files were created from BCL files using bcl2fastq2 v2.18.0.12.[6] FastQC v0.11.4[7] was used to assess the quality of FastQ files. STAR v2.5.3a[8] was used to align each sample's paired-end reads to the Ensembl Mus Musculus reference genome build GRCm38 (using STAR's "2-pass" method). Quality control and assessment of resulting BAM files were performed using QualiMap v2.2.1[9] and RNA-SeQC v1.1.8.[10] Picard v2.0.1[11] was used to add read group information. Aligned files were also processed using Sambamba v0.6.5[12] to mark duplicates and sort reads.

Each sample's BAM file was initially processed using StringTie v1.3.3b[13] and Ensembl gene annotations to guide transcriptome reconstruction. The StringTie option to output "Ballgown-ready" files was enabled.

RNA-seq secondary and tertiary analyses

Using R v3.5.0,[14] Ballgown-ready files were imported into DESeq2 v1.22.2[15] (using tximport v1.10.1[16]) for gene-level exploratory/differential expression analysis. Before performing gene-level exploratory data analyses on r-log transformed data using DESeq2, genes were filtered for exclusion purposes, and removed if the sum of the raw counts for that gene across all samples was less than or equal 1, per guidelines from Love, et al.[17]

Regarding exploratory data analysis (EDA), the following R library packages and functions were used to generate the plots in Supplemental Figure13. All

RNA-seq sample data were r-log transformed. The all-pairs sample comparison displayed in Supplemental Figure 13A utilized an extension to the R package 'ggplot2' called GGally v1.4.0,[18] the Euclidian sample distance heatmap, and hierarchical clustering (Supplemental Figure 13B) used pheatmap v1.0.12,[19] along with Euclidean distances and principal components analysis (PCA). The DESeq2 function plotPCA along with ggplot2 v3.2.0[20] is shown in supplemental Figure 13C, and the hierarchical clustering with heatmap of the top 1000 most variable genes was performed with heatmap.2 (Supplemental Figure 13D), which is the default hierarchical clustering function of gplots v3.0.1.1.[21]

Differential analysis with DESeq2 had no pre-filtering steps. An adjusted *p*-value (q-value) of 0.1 was used as the significance cut off for optimizing the built-in independent filtering performed by DESeq2. In addition, the null-hypothesis tested was set to the default (i.e., the log2 fold change among conditions was zero). Data from this analysis is provided in Supplemental Table 3 "DESeq2 Targets".

To perform Gene Ontology (GO), aka *Biological Processes* subset enrichment/repression analysis, the R library package gProfileR v0.6.7[22] was used. Results are displayed in Figure 6B. Genes that were found significantly overexpressed in the JMML-diseased samples (i.e., had a log2 fold change ≥ 1 and a q-value < 0.1) were submitted to the gProfileR package, using the "strong" hierarchical filtering option. Further, genes that were found to be significantly under-expressed in the JMML-diseased samples (i.e., had a log 2 fold change ≤ -1 and a q-value < 0.1) were submitted in the same manner. The two datasets returned from gProfiler were filtered to include terms with a p-value < 0.5, and then concatenated for further analysis. For each GO term a list of overlapping Ensembl Gene IDs were returned. Additionally for each GO term, the normalized mean count across all genes for a given sample was calculated. Finally, as shown in Figure 6B, the normalized mean counts and GO terms were hierarchically clustered using the heatmap.2 function from the gplots library. Supplemental Table 4 "GO HeatMap Terms & GeneIDs" contains the GO terms along with their corresponding gene targets.

The following procedures were performed in order to analyze the heatmap/hierarchical clustering for Figure 6C, regarding comparison of log2 fold changes of differentially expressed genes found in this study with the data published by Manesia et al[23] (Supplemental Table 5). First, differential analysis was performed on this study's data, using the same *p*-value threshold (p-value < 0.05), q-value threshold (q-value < 0.05), and a log2 fold change threshold (abs[log2FC] ≥ 1) as reported by Manesia et al;[23] second, only genes that were found differentially expressed (given the above thresholds) in both studies and whose log2 fold changes were in the same direction were retained; and finally, the heatmap was generated in R using heatmap.2.

Differentially expressed genes were further analyzed using the Ingenuity Pathway Analysis (IPA).[24] Pathway analysis utilizing cancer canonical signaling pathways for PI3K/AKT, ERK/MAPK, mTOR, and GM-CSF, which were performed using the DESeq2 data set (Supplemental Figure 14**)**. In all cases, JMML vs WT were compared via $\log_2$ fold change. Regarding coloring conventions, red corresponds to up-regulation or overexpression of JMML vs WT, green represents down-regulation or under expression, and grey corresponds to neither up- or down-regulated. The intensity of the color corresponds to the degree of up or down regulation.

Statistical calculation

Differences between groups were evaluated using the nonpararametric Wilcoxon rank sum test or mixed model analysis of variance, which accounted for clustering of animals within litters. A log transformation was applied when data were skewed and to address increasing variability with higher values. For the survival studies, Kaplan-Meier estimates were computed for each group; groups were compared using the log-rank test. Exact 95% binomial confidence intervals were calculated. Data generated from CBC and flow cytometry were expressed as mean ± SE. *P*-values less than 0.05 ($p<0.05$) were considered as statistically significant. Outliers were identified via ROUT analysis (Q=0.5%). Analyses were conducted using SAS 9.3.

References

1. Liu YL, Yan Y, Webster C, et al. Timing of the loss of PTEN protein determines disease severity in a mouse model of myeloid malignancy. *Blood*. 2016;127(15):1912-1922.
2. Peng C, Chen Y, Yang Z, et al. PTEN is a tumor suppressor in CML stem cells and BCR-ABL-induced leukemias in mice. *Blood*. 2010;115(3):626-635.
3. Chang J, Wang Y, Shao L, et al. Clearance of senescent cells by ABT263 rejuvenates aged hematopoietic stem cells in mice. *Nat Med*. 2016;22(1):78-83.
4. Liu YL, Castleberry RP, Emanuel PD. PTEN deficiency is a common defect in juvenile myelomonocytic leukemia. *Leuk Res*. 2009;33(5):671-677.
5. Liu YL, Lensing SY, Yan Y, Cooper TM, Loh ML, Emanuel PD. Deficiency of CREB and over expression of miR-183 in juvenile myelomonocytic leukemia. *Leukemia*. 2013;27(7):1585-1588.
6. Illumina. bcl2fastq2 and bcl2fastq Conversion Software Downloads. Vol. 2018.
7. Babraham Institute BB. FastQC: A Quality Control tool for High Throughput Sequence Data. Vol. 2015.
8. Dobin A, Davis CA, Schlesinger F, et al. STAR: ultrafast universal RNA-seq aligner. *Bioinformatics*. 2013;29(1):15-21.
9. Garcia-Alcalde F, Okonechnikov K, Carbonell J, et al. Qualimap: evaluating next-generation sequencing alignment data. *Bioinformatics*. 2012;28(20):2678-2679.
10. DeLuca DS, Levin JZ, Sivachenko A, et al. RNA-SeQC: RNA-seq metrics for quality control and process optimization. *Bioinformatics*. 2012;28(11):1530-1532.
11. Institute B. Picard. Vol. 2019.
12. Tarasov A, Vilella AJ, Cuppen E, Nijman IJ, Prins P. Sambamba: fast processing of NGS alignment formats. *Bioinformatics*. 2015;31(12):2032-2034.
13. Pertea M, Pertea GM, Antonescu CM, Chang TC, Mendell JT, Salzberg SL. StringTie enables improved reconstruction of a transcriptome from RNA-seq reads. *Nat Biotechnol*. 2015;33(3):290-295.
14. R Core Team RFfSC. R: A language and environment for statistical computing; 2014.
15. Love MI, Huber W, Anders S. Moderated estimation of fold change and dispersion for RNA-seq data with DESeq2. *Genome Biol*. 2014;15(12):550.
16. Soneson C, Love MI, Robinson MD. Differential analyses for RNA-seq: transcript-level estimates improve gene-level inferences. *F1000Res*. 2015;4:1521.
17. Love MI, Anders S, Kim V, Huber W. RNA-Seq workflow: gene-level exploratory analysis and differential expression. *F1000Res*. 2015;4:1070.
18. GGally. Extension to 'ggplot2'. *[*https://CRANR-projectorg/package=GGally*]*.
19. pheatmap:. Pretty Heatmaps [https://CRAN.R-project.org/package=pheatmap].

20. Wickham H. ggplot2: Elegant Graphics for Data Analysis. *New York: Springer-Verlag*. 2016.
21. gplots:. Various R Programming Tools for Plotting Data [https://CRAN.R-project.org/package=gplots].
22. gProfileR:. Interface to the 'g:Profiler' Toolkit [https://CRAN.R-project.org/package=gProfileR].
23. Manesia JK, Franch M, Tabas-Madrid D, et al. Distinct Molecular Signature of Murine Fetal Liver and Adult Hematopoietic Stem Cells Identify Novel Regulators of Hematopoietic Stem Cell Function. *Stem Cells Dev*. 2017;26(8):573-584.
24. IPA. Ingenuity Pathway Analysis [https://www.qiagenbioinformatics.com/products/ingenuitypathway-analysis].

S1

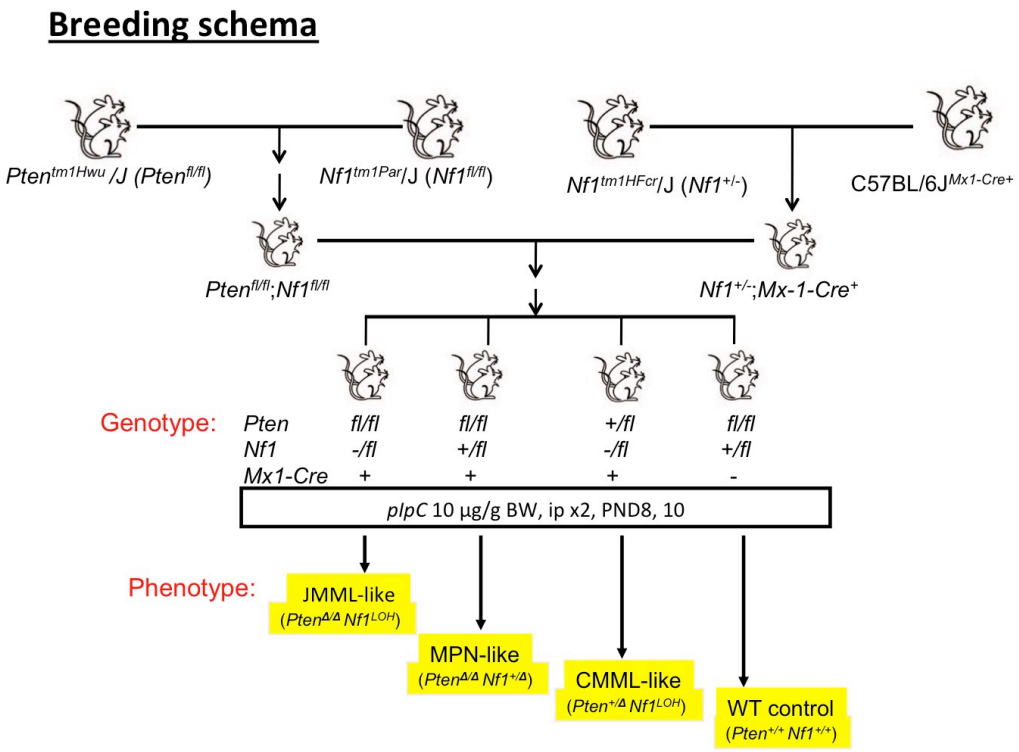

Figure S1. Breeding Schema. *Pten$^{fl/fl}$— Pten$^{floxP/floxP}$; Nf1$^{+/-}$—Nf1$^{Fcr/+}$; Nf1$^{fl/fl}$—Nf1$^{floxP/floxP}$*

S2

Genotypes from Mouse Tails

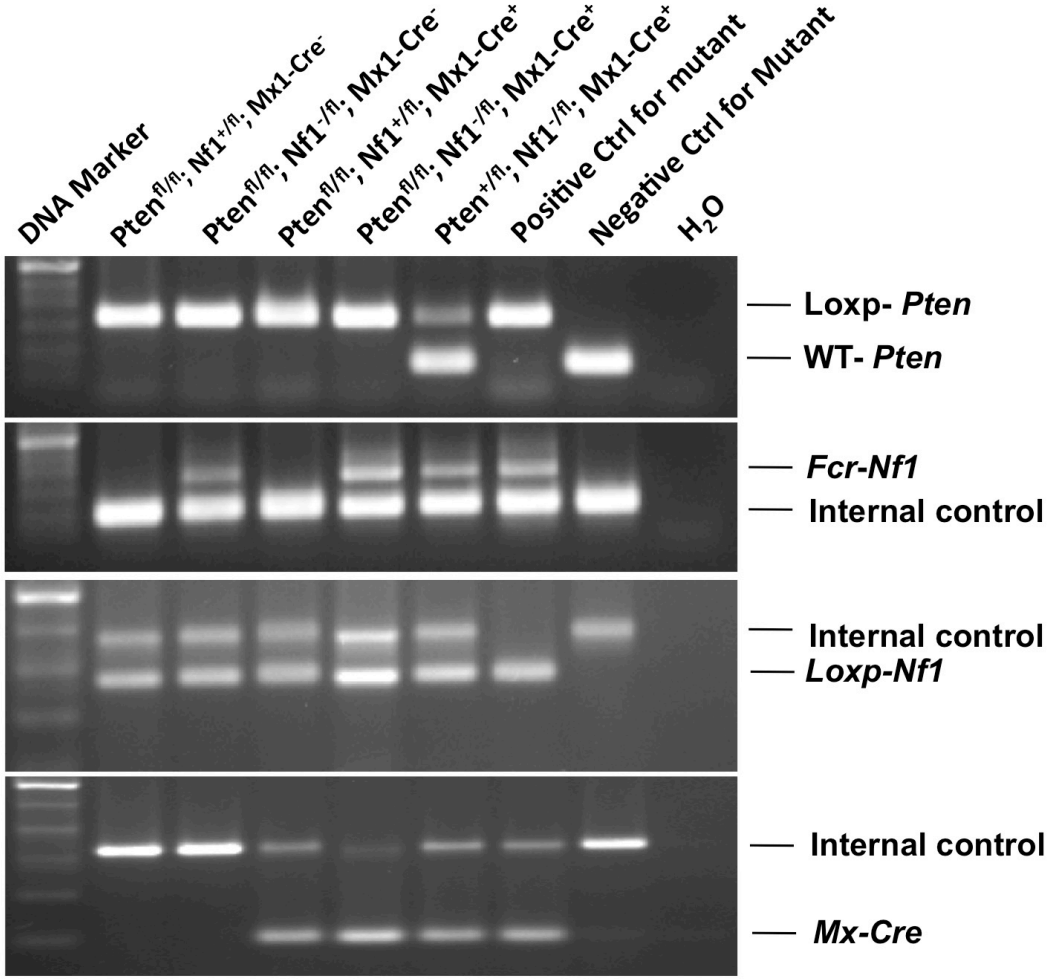

Figure S2: Representative images from genotyping of mice. Mouse tails were clipped at an age of 2 weeks.

S3a

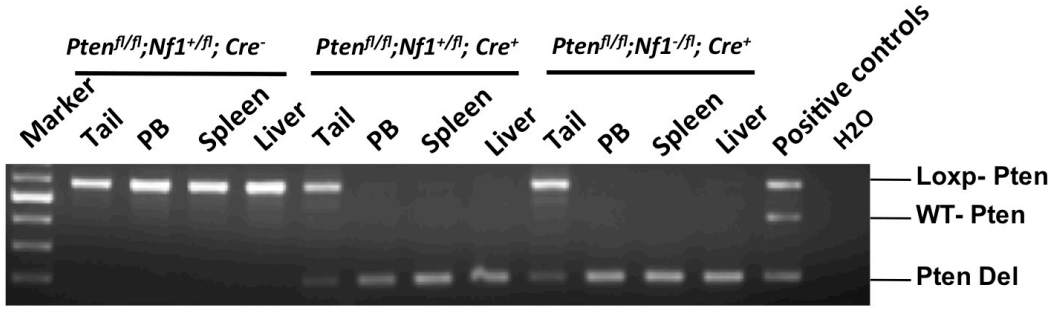

S3b

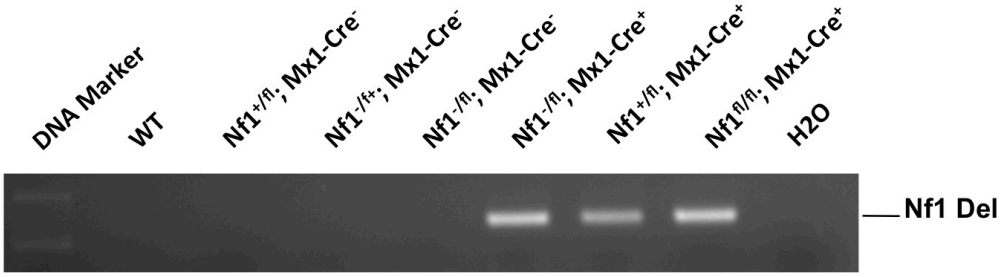

Figure S3. Representative images for genotype analysis by PCR on tissues post deletion inducing. Tissues were collected at age PND18, demonstrating that *Pten* **(a)** and *Nf1* **(b)** were deleted in PB, spleens, and livers in mice with *Mx1-Cre*$^{+}$.

S4a

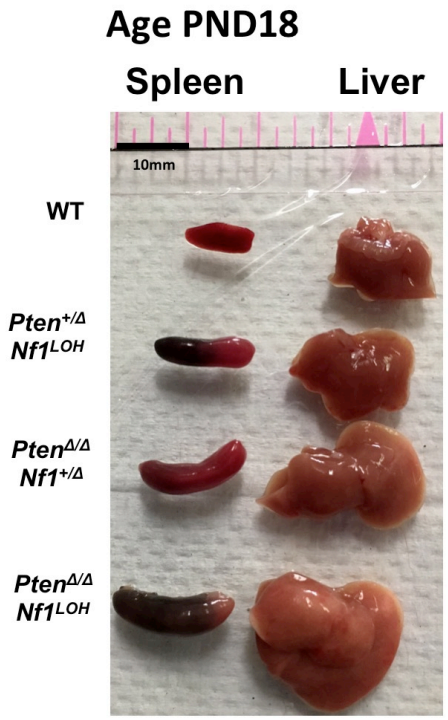

S4b

Figure S4. (a) Photographs of spleens and livers from representative littermate mice at an age PND18. **(b)** Photographs of spleens and livers from representative CMML-diseased mice with *Pten* $^{+/\Delta}$*; Nf1*^{LOH} and age-matched *WT* littermate at an age 3 months. In addition of hepatosplenomegaly, CMML-diseased mice showed bleeding/obstruction of intestine/colon (G/I) due to infiltration of monocyte/macrophage.

S5

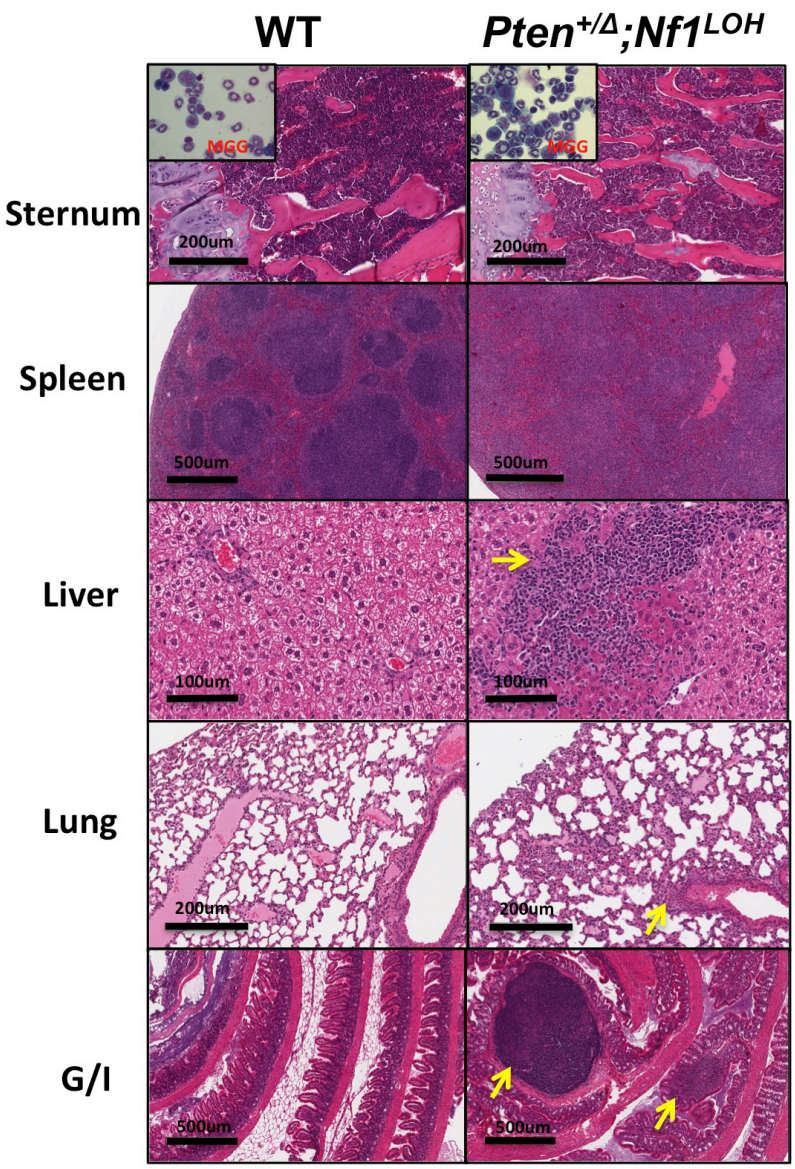

Figure S5: Representative morphological analysis by HE stained tissue sections of formalin-fixed organ tissues from CMML-diseased mice with *Pten*$^{+/\Delta}$*Nf1*^{LOH} and WT littermates at age 3 months. Cytospins from BM show increased granulocytes/monocytes. Substantial infiltrations with granulocytes/monocytes were found in lung, liver, and spleen. Granulocyte/monocyte infiltration involved both red and white pulps of the spleen, which was accompanied by decreased lymphoid tissues. The lungs show nodular infiltration (indicated by an arrow). Granulocyte/monocyte infiltration was observed in the sinuses of the liver (indicated by arrows). Bleeding/obstruction in colon/intestine were due to infiltration of monocyte/macrophage. Images were acquired by a Nikon Eclipse N-V with a 100x lens (BM cytospins) and an Aperio CS2 scanner.

S6

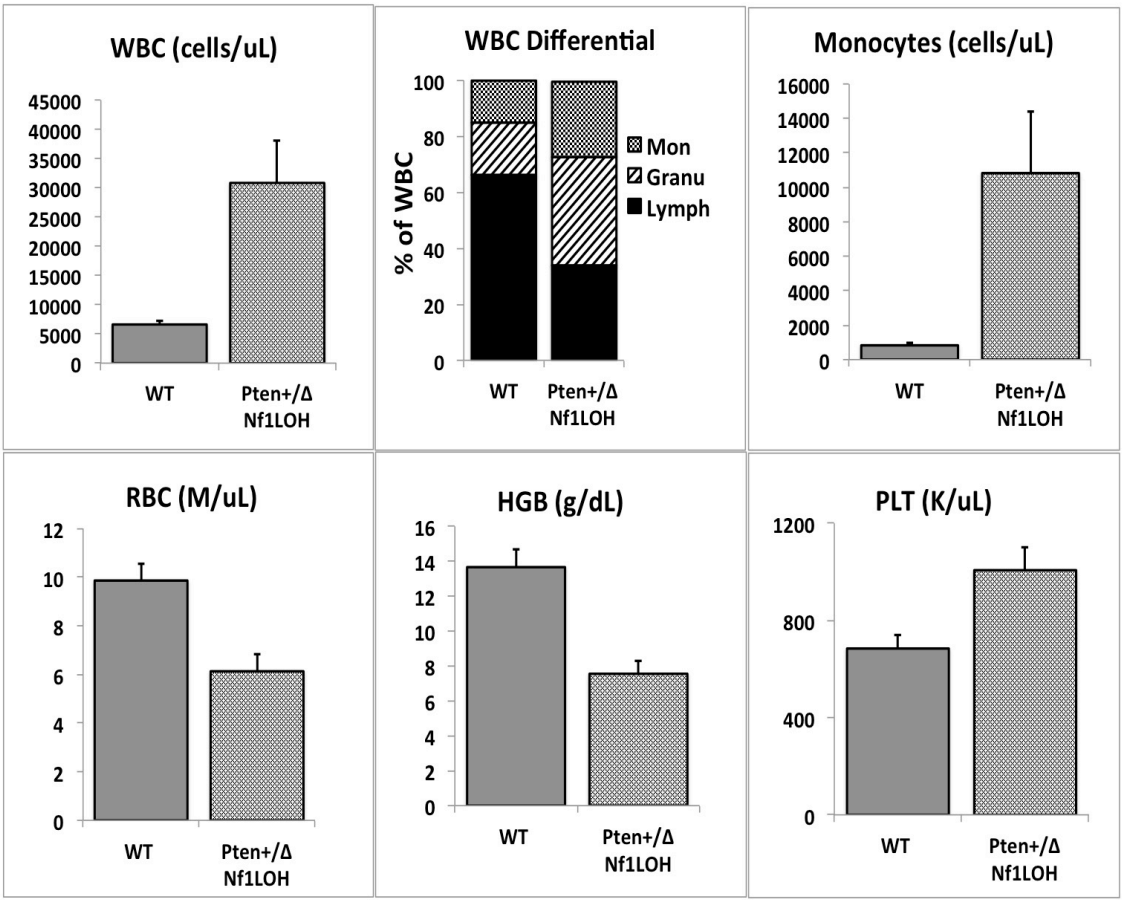

Figure S6: Blood profiles from CMML-diseased mice with *Pten*$^{+/\Delta}$*Nf1*^{LOH} and WT littermates at age older than 3 months when diseased mice were moribund. Complete blood counts (CBCs) were performed with a Vet Abc Hematological analyzer. Differentials were manually counted from blood smears stained with May-Grünwald-Giemsa (MGG). WBC—White blood cell counts, PLT—platelets, RBC—red blood cells, HGB—hemoglobin. Mon—monocytes, Gran—granulocytes, Lymph—lymphocytes. Data are presented as mean ± SE, N=7/each group, p<0.001.

S7

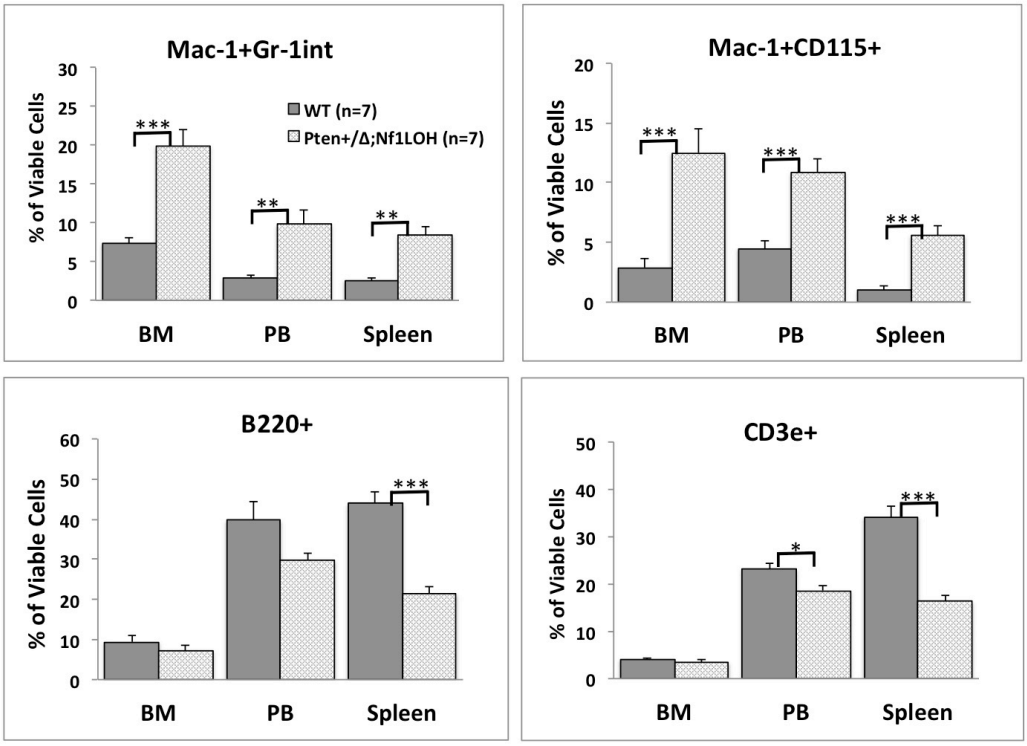

Figure S7: Flow cytometry analysis data from CMML-diseased mice with *Pten*$^{+/\Delta}$*Nf1*^{LOH} and WT littermates at age older than 3 moths when diseased mice were moribund. Data are presented as mean ± SE, *** p<0.001.

S8a

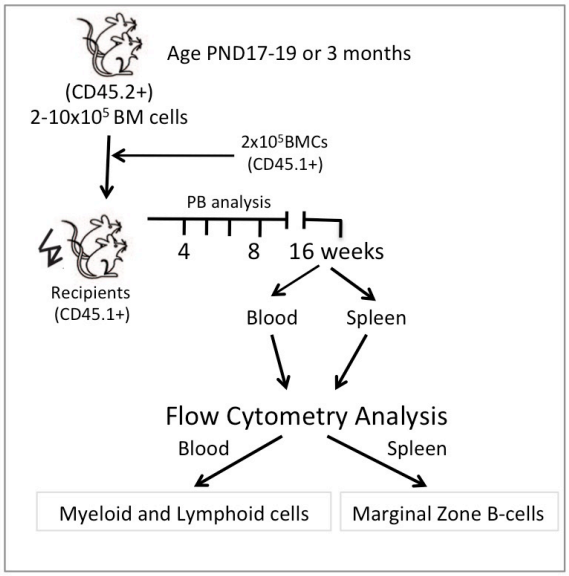

S8b

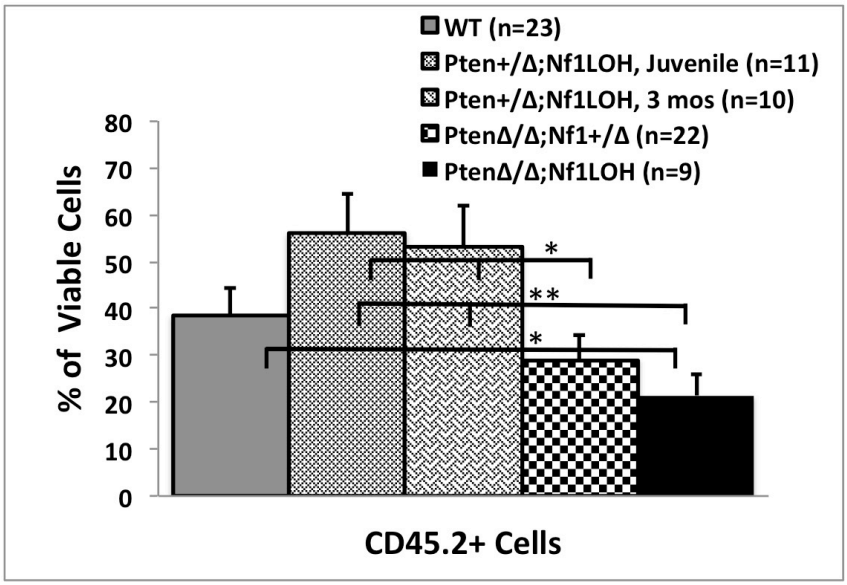

Figure S8. (a) Schema of competitive bone marrow transplantation (BMT). Peripheral blood (PB) and spleen were collected at 12-16th week post-BMT. Engraftments were analyzed by flow cytometry. **(b)** Blood engraftment data. Flow cytometry analyses of PB show the engrafted donor-derived progeny with CD45.2+ in recipients transplanted from juvenile JMML-diseased and littermate donors or 3-month-old donors with *Pten* $^{+/\Delta}$*Nf1* ^{LOH}. Data are presented as mean ± SE, * p< 0.05; ** p<0.01.

S9a

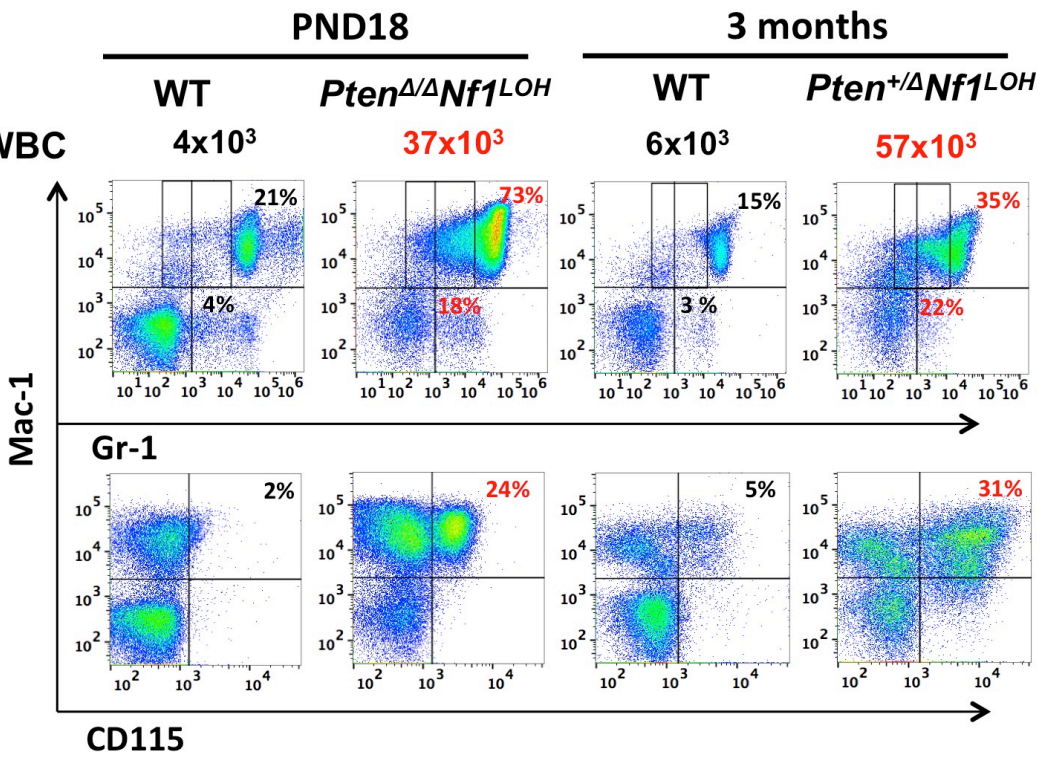

S9b

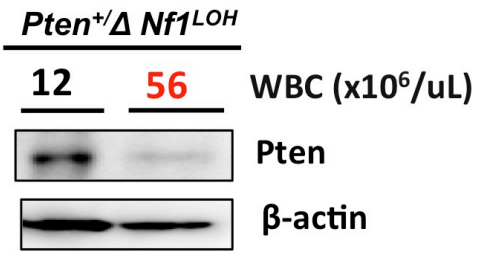

Figure S9. (a) Representative flow cytometry data from blood of JMML- and CMML-diseased mice and age-matched WT littermates. **(b)** Representative western blot data from CMML-diseased adult mice with or without high-WBC. Representative data show that Pten was lost in mice with *Pten*$^{+/\Delta}$ *Nf1*^{LOH} when their WBC reached as high as that in JMML-diseased mice with *Pten*$^{\Delta/\Delta}$ *Nf1*^{LOH}. Data represents 3 experiments.

S10

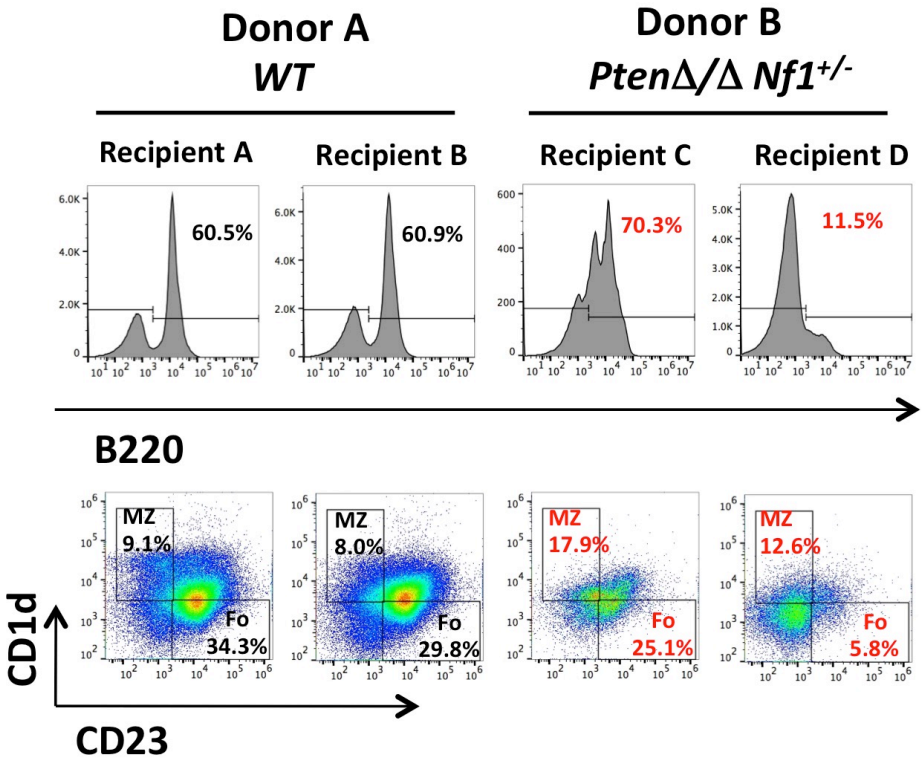

Figure S10. Flow cytometry analysis of spleens from recipient mice transplanted with juvenile donor mice with *PtenΔ/Δ* and germline mutant *Nf1*$^{+/-}$. Representative data demonstrate that juvenile donor BM cells with *PtenΔ/Δ* derive significantly more MZ and fewer Fo B-cells. MZ—donor-derived splenic marginal zone B-cells representing fetal origin of HSCs; Fo—donor-derived follicular B-cells are predominant B-cells in adults.

S11a

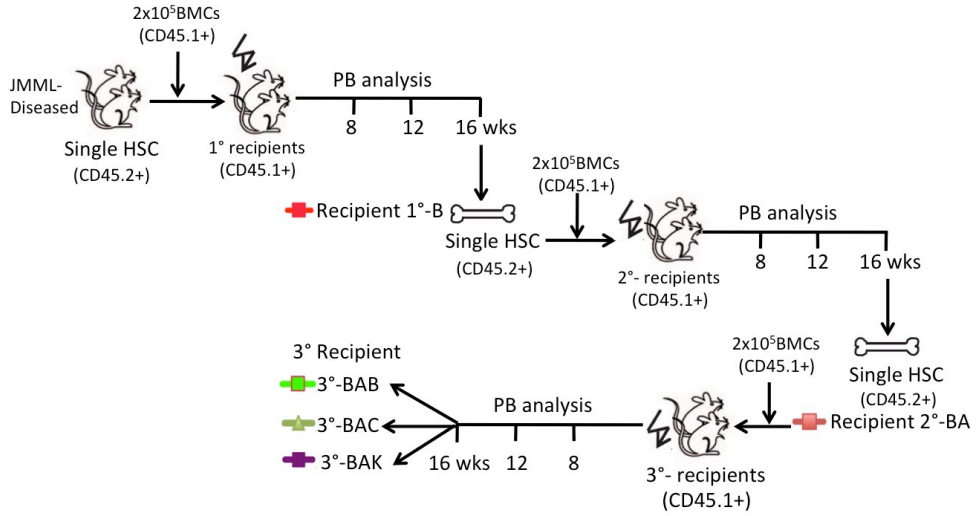

S11b

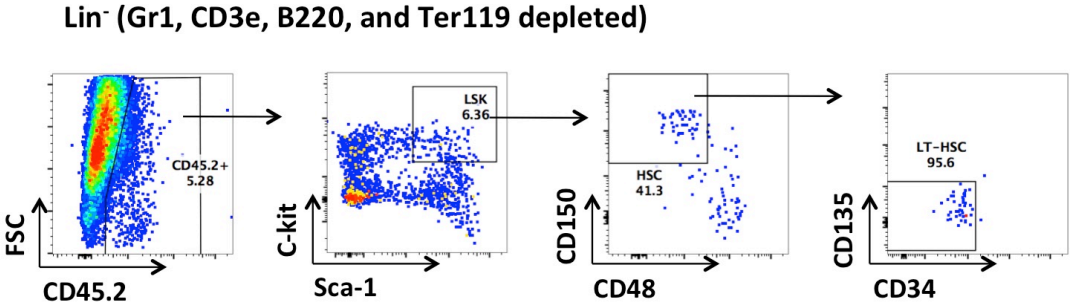

Figure S11. (a) Schema for serial single-HSC transplantation. **(b)** Representative FACS gating strategy for sorting single LT-HSC. Data show representative sorting for LT-HSCs from BM of a primary (1°) transplanted recipient (CD45.1⁺) transplanted with JMML-diseased mice with *Pten*$^{\Delta/\Delta}$ *Nf1*^{LOH} (CD45.2⁺).

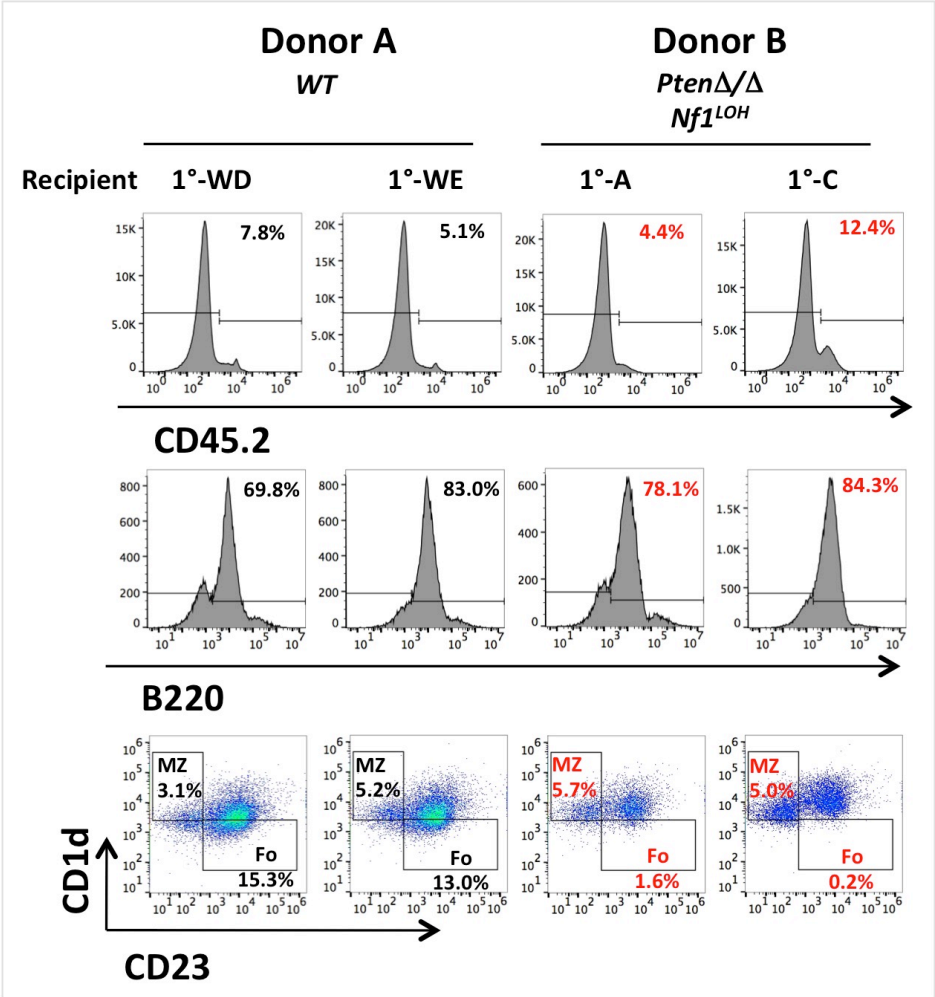

Figure S12. Representative flow cytometry data from spleens of recipients of 1° single-LT-HSC transplants.

S13a

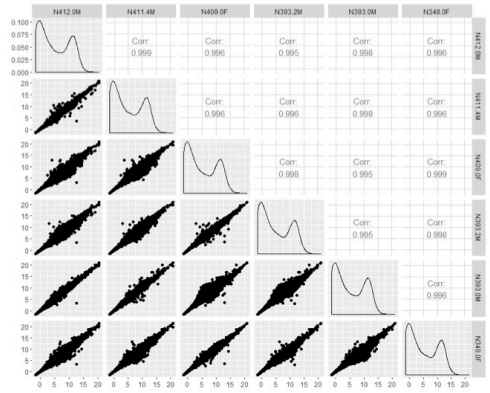

S13b

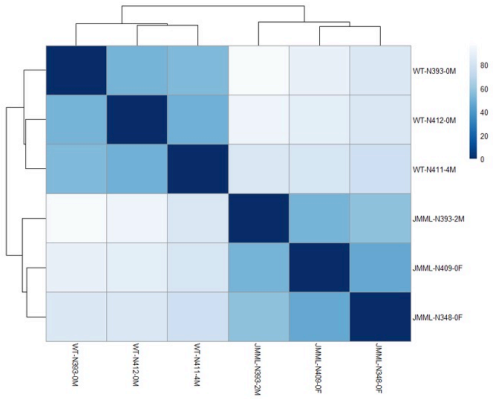

S13c

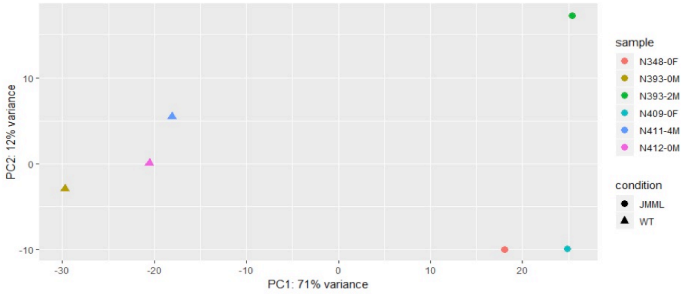

S13d

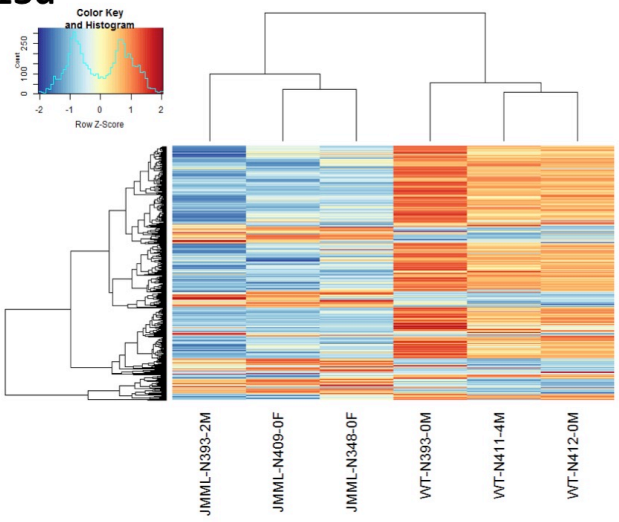

Figure S13. Exploratory data analysis (EDA) using DESeq2. (**a**) All-pairs sample comparisons using r-log transformation (JMML-diseased mice: N348-0F, N409-0F, N393-2M; WT mice: N393-0M, N411-4M, N412-0M). **(b)** Euclidean sample distances heatmap and hierarchical clustering using r-log transformation; (**c**) Principal component analysis using r-log transformation. **(d)** Hierarchical clustering/heatmap of the top 1000 most variable genes using the r-log transformation.

S14a

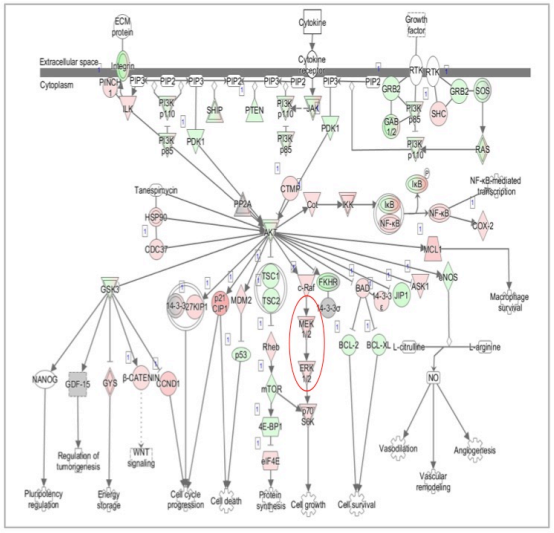

S14b

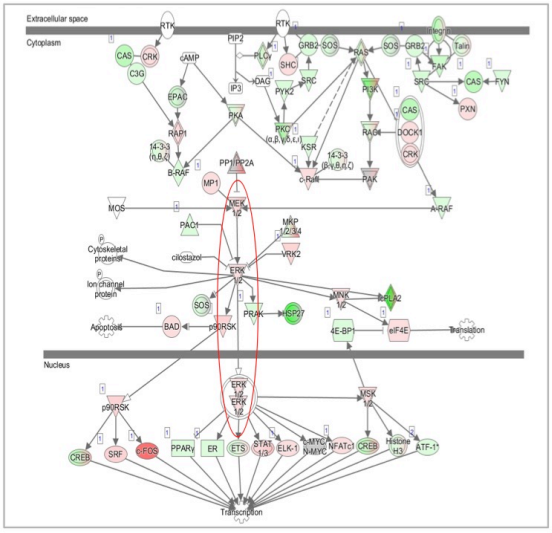

S14c

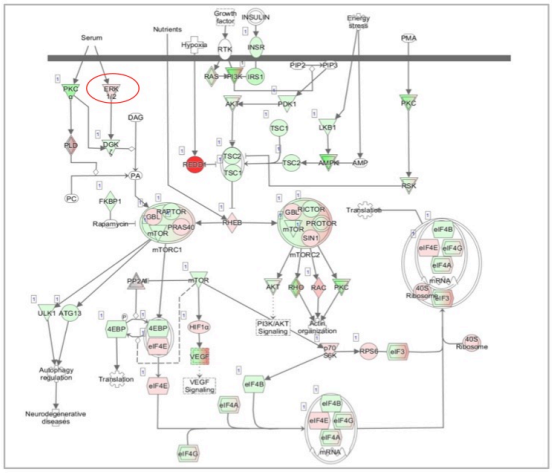

S14d

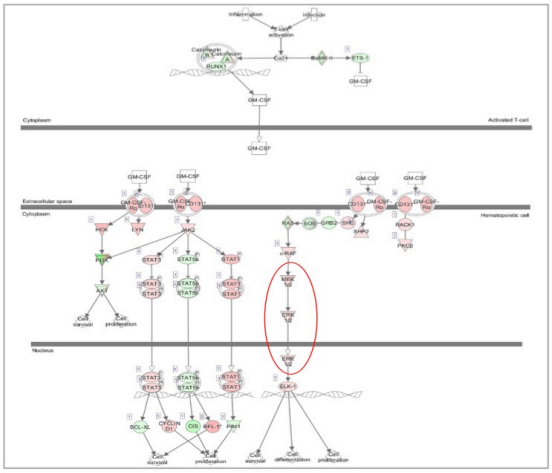

Figure S14: Pathway analysis to compare JMML with WT utilizing cancer canonical signaling pathways for PI3K/AKT **(a)**, ERK/MAPK **(b)**, mTOR **(c)**, and GM-CSF **(d)**, which were performed using the DESeq2 data set. In all cases, JMML vs WT were compared via $\log_2$ fold change. Regarding coloring conventions, red corresponds to up-regulation or overexpression of JMML *vs* WT, green represents down-regulation or under expression, and grey corresponds to neither up- or down-regulated. The intensity of the color corresponds to the degree of up or down regulation. Red circles indicate that MAPK pathway was consistently up-regulated in all 4 analyzed pathways.

Supplemental Table 1: Antibodies for FACS

Name (Clone)	Source	Catalog numbers
APC Rat Anti-Mouse Ly-6G and Ly-6C (RB6-8C5)	BD Biosciences	553129
PE Rat Anti-Mouse CD115 (CSF-1R) (T38-320)	BD Biosciences	565249
PE-Cy 7 Rat Anti-CD11b (M1/70)	BD Biosciences	552850
FITC Hamster Anti-Mouse CD3e (145-2C11)	BD Biosciences	553062
PE Rat Anti-Mouse CD19 (1D3)	BD Biosciences	557399
PE-Cy 7 Rat Anti-Mouse CD45R/B220 (RA3-6B2)	BD Biosciences	552772
PE Rat Anti-Mouse CD71 (C2)	BD Biosciences	561937
APC Rat Anti-Mouse TER-119/Erythroid Cells (TER-119)	BD Biosciences	557909
CD4 Monoclonal Antibody, PE-Cyanine7 (RM4-5)	eBioscience	25-0042-81
APC Rat Anti-Mouse CD8a (53-6.7)	BD Biosciences	553035
FITC Mouse Anti-Mouse CD45.2 (104)	BD Biosciences	553772
Alexa Fluor 647 Rat Anti-Mouse CD23 (B3B4)	BD Biosciences	562826
APC anti-mouse CD34 Antibody (MEC14.7)	Biolegend	119309
FITC Streptavidin	BD Biosciences	554060
APC-Cy 7 Rat Anti-Mouse Ly-6A/E (D7)	BD Biosciences	560654
PE-Cy 7 Rat anti-Mouse CD117 (2B8)	BD Biosciences	561681
BV421 Hamster Anti-Mouse CD48 (HM48-1)	BD Biosciences	562745
PE Rat Anti-Mouse CD135 (A2F10.1)	BD Biosciences	553842
Brilliant Violet 605 anti-mouse CD150 (SLAM) Antibody (TC15-12F12.2)	Biolegend	115927
BV605 Rat Anti-Mouse CD16/CD32 (2.4G2)	BD Biosciences	563006
Brilliant Violet 421 anti-mouse CD127 Antibody (A7R34)	Biolegend	135023
Biotin Rat Anti-mouse CD3e (17A2)	Miltenyi Biotec	130-101-878
Biotin Rat Anti-mouse ly-6G and ly-6C (RB6-8C5)	BD Biosciences	553125
Biotin Rat Anti-mouse CD45R/B220 (RA3-6B2)	BD Biosciences	553085
Biotin Rat Ab-mouse Ter-119/Erythroid cells (TER-119)	BD Biosciences	553672
Dynabeads Biotin Binder	Invitrogen	11047

Supplemental Table 2: Antibodies for western blots

Namce (clone)	Source	Catalog numbers
Anti-PTEN (6H2.1)	Millipore	04-035
phospho-Akt (Ser437) (D9E)	Cell Signaling	4060
Akt (pan) (C67E7)	Cell Signaling	4691
phospho-Erk1/2 (Thr202/tyr204)	Cell Signaling	9101
Erk1/2	Cell Signaling	9102
phospho-S6 Ribosomal protein (Ser240/244)	Cell Signaling	2215
S6 Ribosomal Protein (5G10)	Cell Signaling	2217
Anti-rabbit IgG, HRP-linked antibody	Cell Signaling	20573
Anti-mouse IgG, HRP-linked antibody (from Sheep)	GE healthcare	NA931
β-Actin (AC-15)	Sigma	A5441